Available online at www.sciencedirect.com

ScienceDirect

Current Opinion in Chemical Engineering

Innovative magnetic nanoparticle platform for magnetic resonance imaging and magnetic fluid hyperthermia applications

Xiao Li Liu[1] and Hai Ming Fan[1,2]

Magnetic nanoparticles (MNPs) have been extensively used as contrast and hyperthermia agents for magnetic resonance imaging (MRI) and magnetic fluid hyperthermia (MFH) applications. Current superparamagnetic iron oxides, however, exhibit low sensitivity and poor heating efficiency. MNPs should possess precisely tunable magnetic properties and biological functionalities for early diagnosis and efficient therapeutics, which could be achieved by tailoring the MNP size, shape, composition, and surface coating during chemical engineering processes. Recent advances in controllable synthesis that have helped realize promising MNP platforms as high-performance contrast and hyperthermia agents for highly sensitive MRI and efficient MFH applications have been reviewed. All of those dependences should be optimized together in order to reach a comprehensive, conclusive understanding of MNPs and maximize T_1 or T_2 relaxivity and specific absorption rate (SAR) to chemically engineer an ideal nanoagent.

Addresses
[1] School of Chemical Engineering, Northwest University, Xi'an, Shaanxi, 710069, China
[2] State Key Lab Incubation Base of Photoelectric Technology and Functional Materials, Northwest University, Xi'an, 710069, China

Corresponding author: Fan, Hai Ming (fanhm@nwu.edu.cn)

Current Opinion in Chemical Engineering 2014, **4**:38–46

This review comes from a themed issue on **Nanotechnology**

Edited by **Hong Yang** and **Hua Chun Zeng**

Available online XXX

2211-3398/$ – see front matter, Published by Elsevier Ltd.

http://dx.doi.org/10.1016/j.coche.2013.12.010

Introduction

The use of magnetic materials in medicine has a long history [1] and has been largely stimulated by the emergence of superparamagnetic nanoparticles (NPs). Due to their unique magnetic properties and comparable size to functional biomolecules, magnetic nanoparticles (MNPs) have been considered as one of the most promising materials for biomedical applications. [2] With increasing demand in effectual treatment and noninvasive, real-time disease diagnosis, MNPs can enhance magnetic resonance imaging (MRI) sensitivity, magnetic heating efficiency, and deep tissue penetration of the magnetic field, making MNPs particularly attractive for constructing high-performance contrast/hyperthermia agents for diagnostic and therapeutic applications [3,4].

MNPs find application as contrast agent in MRI, a diagnostic technique based on the difference between the nuclear magnetic relaxations of water protons in biological solutions and around solid tissues. Contrast agents shorten the relaxation times (T_1 and T_2) that characterize the two independent processes of proton relaxation. T_1 describes the spin–lattice or longitudinal relaxation generating a bright image, whereas T_2 specifies the spin–spin or transverse relaxation of the excited protons, resulting in a dark image. Contrast-agent efficiency is usually measured through relaxivity, r_1 or r_2 ($mM^{-1}\,s^{-1}$) [2]; higher relaxivity corresponds to a better contrast effect. Magnetic hyperthermia, also known as magnetic fluid hyperthermia (MFH), is a novel concept in cancer treatment. It is based on the evidence that cancer cells are more sensitive than normal cells to temperatures higher than 41°C. The conversion of electromagnetic energy into thermal energy under externally applied alternating magnetic field (AMF) by MNP colloid mediator is mainly attributed to the Brownian-Néel relaxation loss of MNPs. The production of thermal energy is continuously measured in terms of specific absorption rate (SAR, $W\,g^{-1}$) [5•,6]. The applied field should be below $5 \times 10^9\,Am^{-1}\,s^{-1}$ and the frequency limited to $\leq$1 MHz [7,8] to minimize possible side effects. Despite MRI and MFH being different biomedical applications, they share some common requirements for MNPs to maximize MR T_2 relaxivity and SAR such as large saturation magnetization (M_s) and susceptibility. Further, combining MRI and magnetic hyperthermia treatment, referred to as 'theranostics' [9], could allow control over the treatment efficacy in a large degree.

Despite the stated advantages of MNPs, the main challenges to their use from bench to bed are low MR sensitivity and relatively poor energy transfer efficiency. As illustrated in Figure 1, a typical contrast/hyperthermia agent is a system comprising two key components: magnetic core and coating shell. In order to improve the performance of nano-agents, significant effort has been dedicated on the preparation of MNPs to control the size, shape, composition, surface functionalization, and magnetic properties of MNPs [10••,11,12]. Preparing a desired nanoagent system would be much more complicated if we further considered the interparticle interactions, core–shell interface, and their synergistic effects, if any. This mini-review identifies critical issues

Figure 1

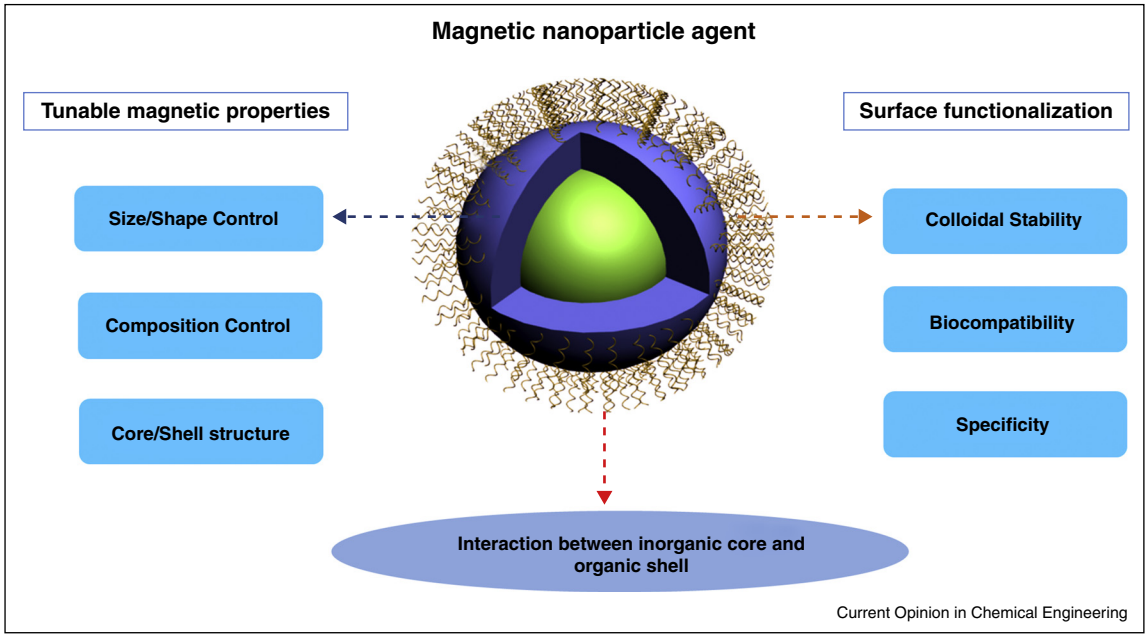

Illustration of representative NP agent comprised of magnetic core and shell coating for biorelated applications.

and newly available strategies for controlling synthesis of MNPs and modifying MNP surfaces to significantly improve their performance as contrast/hyperthermia agents. Since iron oxide NPs show excellent biocompatibility, this article describes ferrite NP cores and biocompatible shells. The highlighted topics may open new frontiers for advanced research of nanochemical engineering.

MNP preparation methods

The controllable synthesis of highly monodisperse magnetic nanocrystals is a key for biomedical applications. Numerous MNP synthesis methods including coprecipitation [13], sol–gel synthesis [14], microemulsion synthesis [15], sonochemical reaction [16], hydrothermal reaction [17], thermal decomposition [18••], hydrolysis synthesis [19], and laser pyrolysis [20] have been developed so far. The preferred method for preparing monodisperse NPs involves thermally decomposing iron salts in high-temperature organic solutions. A suitable surfactant is used either as a capping agent to stabilize such NPs or as a structure-directing molecule to control nanocrystal morphology. Because it can reliably achieve the separation of the nucleation and the growth of nanocrystals, this method affords significant control over particle size, shape, crystallization, and composition. However, the decomposition of the precursors occurs at high temperatures (e.g. ferric oleic decomposes above 200°C), thereby consuming large amounts of energy and increasing the thermal requirements of reactor systems during industrial production. Therefore, growth of magnetic ferrites at room temperature by co-precipitation or hydrolysis of iron salts from aqueous solutions is favored for large-scale chemical production, for it has benefits of low cost and high feasibility. However, using these methods to precisely control the required specifications requires further investigation.

Controlling size and shape of MNP agent

Magnetism originates from electron spins and movement [21]. NP magnetic properties are strongly associated with NP size and shape. To minimize the energy, ferromagnetic NPs split into domains in which all dipoles are ordered along a preferential direction. The magnetization directions can be aligned by an external field (H) to achieve saturation magnetization (M_s) [22]. The ease at which a ferromagnet/ferrimagnet can be aligned is measured by its susceptibility (M/H). As illustrated in Figure 2a, the magnetization remaining at zero field and the field strength required for demagnetization are defined as remnant magnetization (M_r) and coercivity (H_c), respectively. The coercivity is dependent on particle size as shown in Figure 2c. There is a critical size below which it costs more energy to create a domain wall than to support the external magnetostatic energy of the single-domain state. Above the critical size, multidomain magnetism begins in which a smaller reversal magnetic field is required to make the net magnetization zero. Generally, at the size smaller than 20 nm for spherical NPs, a ferromagnetic NP often contains a single domain. As the size of these single domain particles decreases, the coercivity decreases. When ferromagnetic NP size is

Figure 2

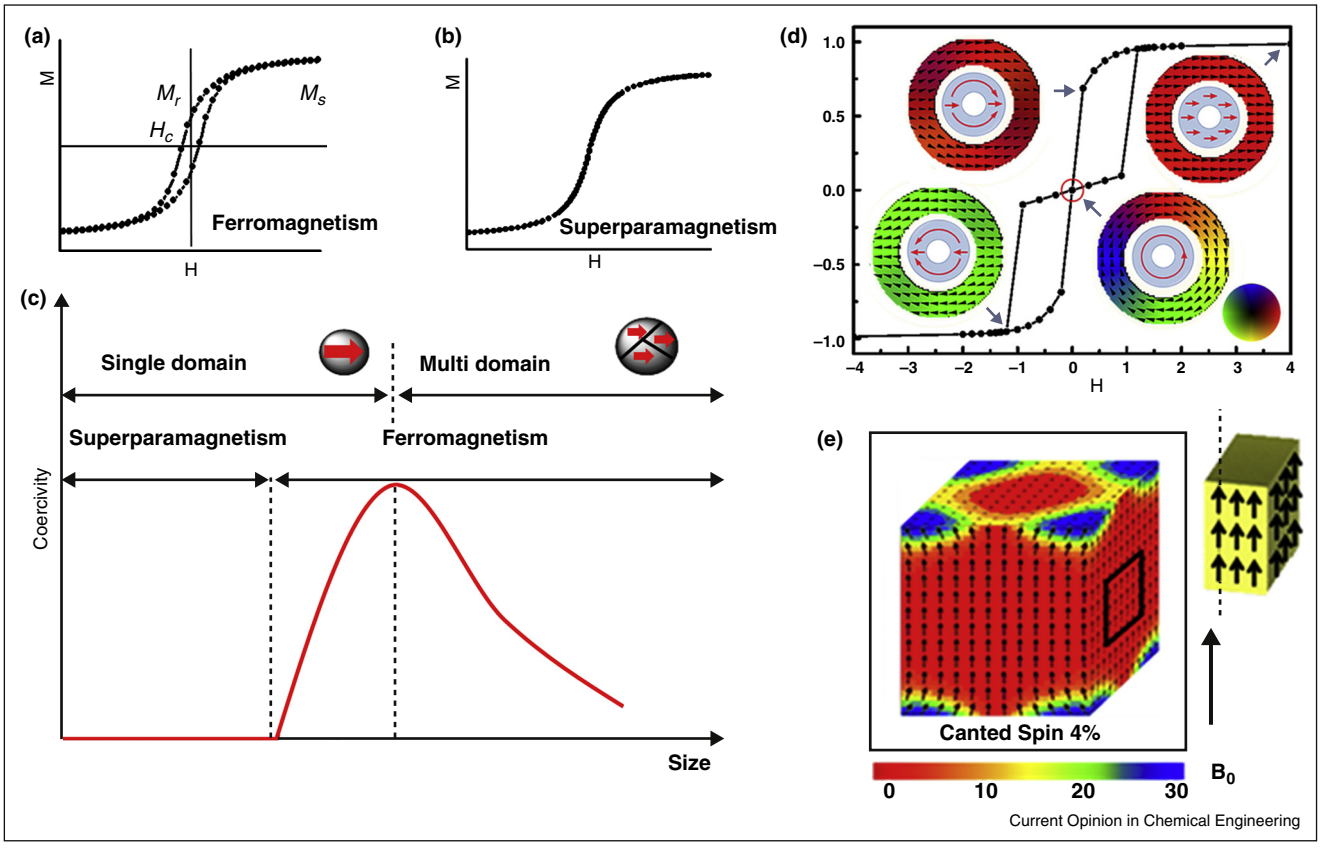

Hysteresis loop for **(a)** ferromagnetic NPs and **(b)** superparamagnetic NPs. **(c)** Size-dependent H_c. **(d)** Hysteresis loops simulated for magnetite nanorings in vortex region at D_{out} = 70 nm with T = 50 nm in ground-state phase diagram. Insets show field direction and snapshots during transition [56]. Reprinted with permission from [56]; Copyright 2012, AIP Publishing, LLC. **(e)** Magnetic spin states simulated using object-oriented micromagnetic framework (OOMMF) program for cube. Color map indicates degree of spin-canting against external magnetic field (B_0), where red indicates nondeviated spins and blue indicates highly canted spins. Local spin states on NP surfaces are depicted at the right corners. Cube exhibits 4% lower spin disorder [57]. Reprinted with permission from Ref. [57]; Copyright © 2012, American Chemical Society.

continually decreased to a level where the magnetic anisotropy energy (KV, K is bulk magnetocrystalline anisotropy, V is NP volume) is smaller than the thermal energy (k_BT, k_B is the Boltzmann constant, T is temperature), the MNP is said to be superparamagnetic [23]. At superparamagnetic state, MNP shows no H_c or M_r; thus, the magnetic dipole–dipole interaction is minimized (Figure 2b). MNPs tend to become paramagnetic when their size is decreased even. MNPs should be designed to show small M_r and H_c thereby facilitating stable colloid formation, which is very important for biomedical applications.

Iron oxide NPs usually serve as a T_2 contrast agent whose relaxivity depends on $(M_sV)^2$, where V represents NP volume [3,24]. Therefore, relatively large NPs showing large M_s are desirable for use as highly sensitive MRI contrast agents. Size-controlled synthesis of monodisperse iron oxide NPs has been widely studied [25,26]. MNP size can be tuned by varying the growth temperature from 260 to 320°C during thermal decomposition, in which metal acetylacetonate [26] or metal oleate [25] are frequently used as precursors. Synthesizing Fe_3O_4 NPs from iron acetylacetonate at 265°C can produce 4 nm NPs, while synthesizing iron oxide NPs from the iron oleate precursor produces 5–22 nm monodisperse iron oxide NPs. Larger Fe_3O_4 NPs can also be produced through seed-mediated growth. Nanoclusters are another kind of aggregated ultrasmall NPs. It can provide large particle size up to thousands of nanometers while retaining superparamagnetic behavior, thus exhibiting the superhigh T_2 relaxivity for single particle imaging [27]. Recent interesting findings in this area are the preparations of extremely small iron oxide NPs as T_1 contrast agents. A series of experiments has demonstrated that ferrite NPs smaller than 5 nm can exhibit large r_1 and low r_2/r_1, thereby exhibiting the suitable relaxometric property of a T_1 contrast agent [19,28••,29••]. Tromsdorf *et al.* [29••] fabricated 4 nm phosphate-poly-(ethylene glycol) (PEG) modified iron oxide NPs whose r_1 (r_1 = 7.3 mM^{-1} s^{-1} and r_2/r_1 = 2.4) at 1.41 T is two times

higher than those of commercial Magnevist®, a typical T_1 contrast agent. Kim *et al.* [28••] recently modified a thermal decomposition method where oleyl alcohol was used to lower the reaction temperature by reducing an iron-oleate complex, resulting in the large-scale production of <4 nm iron oxide NPs showing $r_1 = 4.78\ mM^{-1}\ s^{-1}$ for 3 nm NPs at 3 T and longer circulation time, thus enabling high-resolution imaging. Small-sized ferrite NPs such as $ZnFe_2O_4$ and $NiFe_2O_4$ NPs also show similar behavior [19]. Designing MNP agents for MFH applications follows size optimization and selection criteria similar to those for MRI applications because the SAR of MNPs is also proportional to M_s^2 [5•]. That is, large NPs showing high M_s exhibit better SAR. However, SAR may show a maximum at a certain particle size near the transition from single-domain to multi-domain [30•]. It is noteworthy that Brownian relaxation can be particularly important for colloid MNPs contributing ~50% of total heat energy for 10 nm superparamagnetic iron oxides (SPIO) [31]. However, once MNPs are internalized by or attached to cells, the physical rotation of the MNPs is confined, and the intrinsic moment rotation dominates MNP relaxation, significantly reducing SAR in practical applications [32]. In addition, nanoclusters that could improve T_2 relaxivity in MRI applications are not favored for magnetic hyperthermia because NP aggregation largely decreases the SAR [33].

Besides the size, tuning shape of MNPs in nano-scale offers additional degree of freedom in optimizing the magnetic properties of NPs. Various MNPs including nanorods, nanowires, nanocubes, hollow nanorings, and nanotubes have been developed [34–36]. Nanorings and nanocubes exhibiting unique magnetic properties are particularly interesting for MRI and MFH applications. Fe_3O_4 nanorings can be obtained by reducing Fe_2O_3 nanoring templates prepared through coordinate dissolution process in hydrothermal condition [35,36]. Figure 2d shows simulated hysteresis loops of magnetite nanorings at outer diameter $D_{out} = 70$ nm; thickness $T = 50$ nm in the vortex region of the ground-state phase diagram. Unlike spherical NPs, the nanorings with specially tailoring dimension could exhibit stable vortex state with minimal external stray fields where magnetic flux circulates around it [37]. Therefore, the overall magnetic moment of each nanoring is zero in the absence of an external field, and the magnetic attraction between the NPs can be negligible for magnetic nanoring colloids. Quantum dot capped ferrimagnetic vortex-state iron oxide (QD-FVIO) magnetized under small external fields will quickly align along the field direction, transitioning from the vortex state to the onion state and reaching its maximum [38••]. *In vitro* MRI measurements have indicated that biocompatible vortex nanorings show much stronger magnetic resonance (MR) T_2^*, where the r_2^* relaxivity and r_2^*/r_1 are 4 and 110 times larger, respectively, than those of a commercial SPIO contrast agent [38••]. Magnetic iron oxide nanocubes ranging from 20 to 160 nm can be synthesized by kinetically controlling a high monomer concentration during thermal decomposition [39]. Such nanocubes are enclosed by a flat surface showing a low-energy {1 0 0} family facet, resulting in less disordered surface spin (Figure 2e) and larger M_s than spherical MNPs. At the same time, the coercivity and remnant magnetization are very small to prevent strong magnetic dipole interaction. The r_2 relaxivity of 22–28 nm Fe_3O_4 nanocubes is up to $761\ mM^{-1}\ s^{-1}$ at 3 T and did not increase with increased size [40••]. The high M_s provided by nanocube also facilitates high SAR in MFH. Guardia *et al.* used cubic iron oxide nanocrystals for cancer cell hyperthermia treatment [41••]. The 19 nm Fe_3O_4 nanocubes reached a SAR value of 2277 W/g Fe (700 kHz and 24 kA m^{-1}) and 1000 W/g Fe (325 kHz and 22 kA m^{-1}), much higher than spherical NPs (~300 W g^{-1}).

Controlling composition of MNP agent

MNP composition plays a critical role in determining the magnetic properties; therefore, manipulating composition provides more opportunities to tailor the property. The newly designed MNPs are mainly composed of doped, alloy, core–shell, and multilayered nanostructures which can be prepared by mixing different metal salt as precursors or seeded growth in high-temperature organic solution. One of the simplest methods of engineering MNPs is to change the chemical identity of M^{2+} because metal ferrites (MFe_2O_4) have oxygen-packed, face-centered cubic lattices where metal ions (M^{2+} and Fe^{3+}) occupy either tetrahedral (T_d) or octahedral interstitial (O_h) sites. For example, substituting Fe^{2+} with magnetic atoms such as Mn, Co, and Ni changes the magnetic spin moment from 4 to 5, 3, and 2 μB, respectively. $MnFe_2O_4$ shows the highest mass magnetization (~110 emu/g, 12 nm); thus, it showed considerably enhanced MR sensitivity for cancer cell detection [10••]. Cheon *et al.* [42••] also demonstrated that the efficiency of MR contrast and hyperthermia agents can be effectively modulated by Zn^{2+} dopant control. Substituting Fe^{2+} with nonmagnetic Zn^{2+} (0 μB) in the T_d holes reduces the antiparallel spin interactions between the magnetic ions in the O_h holes and T_d holes, increasing the net magnetization of the NPs (Figure 3a). The modulation of M_s directly generates enhanced contrast effects where the r_2 increases significantly from less than 100 to almost $700\ mM^{-1}s^{-1}$ as seen in Figure 3b. Similarly, the measured SAR is 4 times greater than that for conventional NP agents used for hyperthermia cancer cell treatments (Figure 3c). Constructing inorganic core/shell structures with controlled dimensions is another strategy to tune magnetic properties of MNPs. The advantage of such core/shell NP systems is that their magnetic properties can be tuned by controlling the core diameter and shell thickness [43•]. Liu and Sun synthesized $Fe_{58}Pt_{42}/Fe_3O_4$ core/shell nanocomposite by using FePt NP as seeds and subsequently

Figure 3

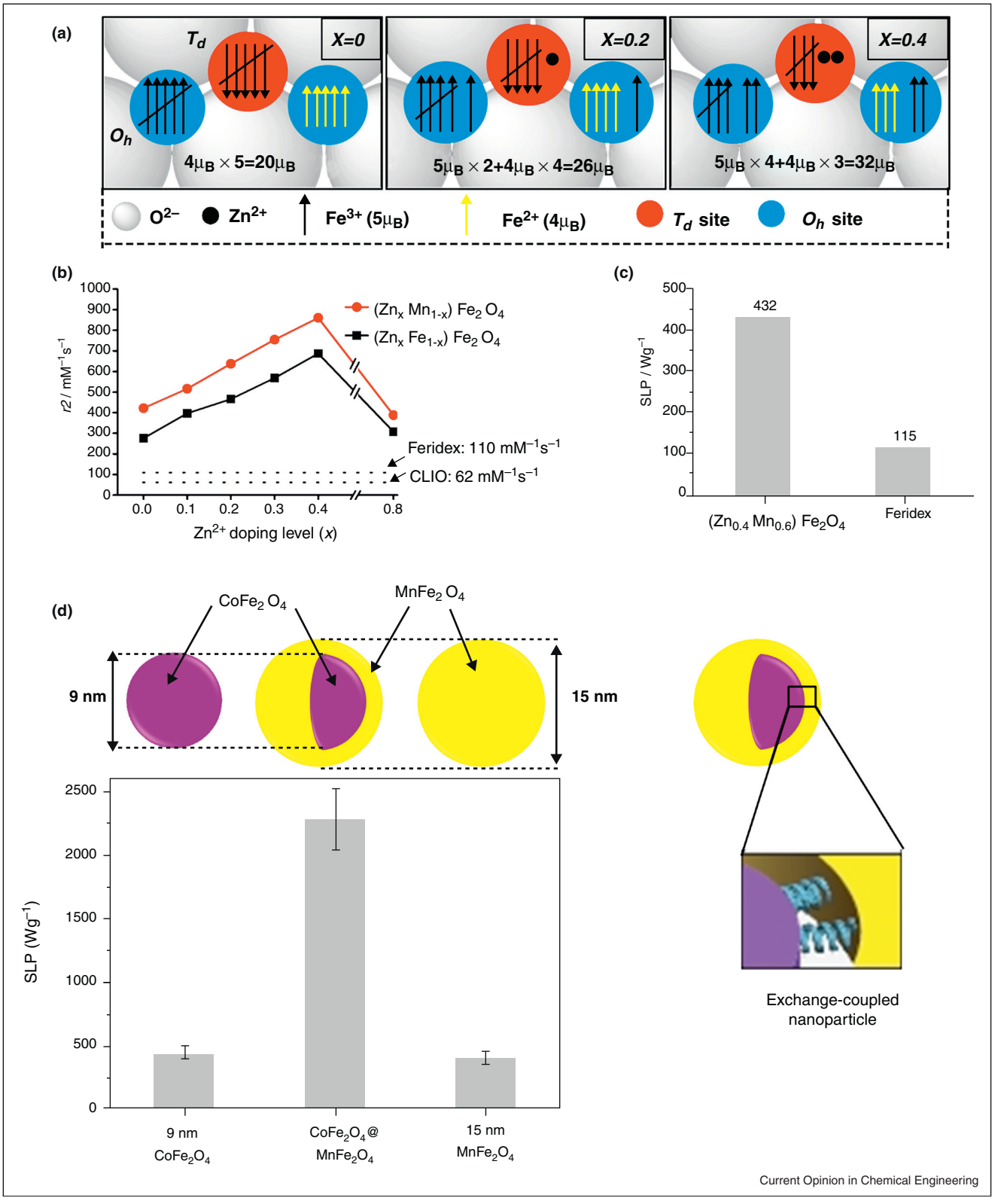

(a) Magnetic-spin-alignment diagrams for undoped, Zn^{2+} doped ($x = 0.2$), and Zn^{2+} doped ($x = 0.4$) spinel-structured $(Zn_xFe_{1-x})Fe_2O_4$ NPs under applied magnetic field. **(b)** Graphs of r_2 versus Zn^{2+}-doped $(Zn_xFe_{1-x})Fe_2O_4$ (M = Mn^{2+}, Fe^{2+}) NPs at 4.5 T [42••]. Copyright © 2009 Wiley–VCH Verlag GmbH & Co. KGaA, Weinheim. **(c)** SLP values for $(Zn_{0.4}Mn_{0.6})Fe_2O_4$ and Feridex in a 500 kHz AC magnetic field with an amplitude of 3.7 kA m^{-1} [42••]. Copyright © 2009 Wiley–VCH Verlag GmbH & Co. KGaA, Weinheim. **(d)** (Left) Schematic representation of 15 nm $CoFe_2O_4$@$MnFe_2O_4$ NP and its SLP compared with those for its components (9 nm $CoFe_2O_4$ and 15 nm $MnFe_2O_4$); (Right) Schematic representation of core–shell NP showing exchange-coupled magnetism [44••]. Copyright © 2011, Rights Managed by Nature Publishing Group.

Table 1

T_1 or T_2 relaxivities of contrast agents with different surface coating

Core	Surface coating	Core size (nm)	Hydrodynamic size (nm)	T_1 relaxivity ($mM^{-1}\,s^{-1}$)	T_2 relaxivity ($mM^{-1}\,s^{-1}$)	Magnetic field (T)
Fe_3O_4-14 [50••]	DSPE-mPEG1000	14	28.6		385	7
Fe_3O_4-14 [50••]	DSPE-mPEG5000	14			151	7
Fe_3O_4-5 [50••]	DSPE-mPEG1000	5	14.8		130	7
Fe_3O_4-5 [50••]	DSPE-mPEG1000	5			30	7
Alkynyl-DOTA-Gd [52]				3.12		1.5
H40-PCL-b-P(OEGMA-Gd-FA) [52]			28.5	18.14		1.5
Endorem® [53]	Dextran T10		120–180		141	1.5
NPsco@1 [53]	Compound 1		50		272	
NPsco@3 [53]	Compound 3				213	
Resovist® [53]	Carboxydextran		60		188	1.5
Magneto liposome [53]	PEG-liposomes		40		240	1.5
$MnFe_2O_4$ [54]	PEO-PEI	3	15		43	3
$MnFe_2O_4$ [54]	PEO-PEI	9	30		57	3
$MnFe_2O_4$ [54]	PEO-PEI	18	40		107	3
$MnFe_2O_4$ [54]	Encapsulated	4.5			32	3
$MnFe_2O_4$ [54]	Encapsulated	6			53	3
$MnFe_2O_4$ [54]	Encapsulated	7.5			77	3
$MnFe_2O_4$ [54]	Micelles	4.5			94	3
$MnFe_2O_4$ [54]	Micelles	6			122	3
$MnFe_2O_4$ [54]	Micelles	7.5			196	3
$MnFe_2O_4$ [54]	Micelles	9			167	3
Resovist® [54]			60		260	3
Fe_3O_4 [49••]	PMO	10	14–5	7.8	27.2	1.5
Fe_3O_4 [49••]	PEG-g-PEI	10	25	11.2	39.8	1.5
Fe_3O_4 [49••]	PEI	10	14–5	21.5	75.2	1.5
Fe_3O_4 [49••]	PMO	30	44–5	10.9	70.5	1.5
Fe_3O_4 [49••]	PEG-g-PEI	30	56.6	39.8	93.3	1.5
Fe_3O_4 [49••]	PEI	30	44–5	29	107.3	1.5
Fe_3O_4 [27]	PBMA-g-(C12/Fluorescein)	6	20.2		101	3
Ferucarbotran [27]			62		238	3
Fe_3O_4 MNNA [55]		40	90		314.6	3
Fe_3O_4 [55]	2,3-Dimercaptosuccinic acid	6	17		196.7	3
Ferumoxytol [55]			25		84.9	3

grew Fe_3O_4 in phenyl ether at 265°C. This nanocomposite contains the direct contacted $Fe_{58}Pt_{42}$ hard phase and Fe_3O_4 soft phase, leading to strong exchange coupling. Lee *et al.* developed a family of exchange-coupled core/shell ferrite NPs for efficient heat induction, as shown in Figure 3d. The $Zn_{0.4}Co_{0.6}Fe_2O_4$@$Zn_{0.4}Mn_{0.6}Fe_2O_4$ core–shell NPs exhibited the highest M_s (150 emu/g) and attained the highest specific loss powers among the NPs, 3886 W g^{-1}, 34 times larger than those for conventional iron oxide NPs [44••]. Animal studies have demonstrated a 75 μg dose of the NPs during magnetic hyperthermia treatment could effectively eliminate tumors.

Surface functionalization of MNP agent

Monodisperse inorganic magnetic NPs grown in organic solution with controlled shape and size are usually capped with a long-chain hydrocarbon, leading to a hydrophobic surface. To make these NPs for biological applications, their surfaces are usually functionalized accounting for high colloidal stability, specificity and biocompatibility. Various materials have been used to coat magnetic NPs. For example, dopamine was found to be a stable anchor on the Fe_3O_4 NP surface [45]. Polyethylene glycol (PEG), chitosan, dextran, and poly(acrylic acid) (PAA) could be used to stabilize nanostructures and offer long-term stability and biocompatibility [46,47]. Antibodies (and their fragments), lectins, proteins, hormones, charged molecules and some low molecular weight ligands such as folate were associated with magnetic NPs to enhance target specificity [48]. Table 1 summarizes the direct effect of surface coating optimization on relaxivities. Except for functionalization of magnetic core, the surface coatings directly affect MRI and MFH performance. Nie *et al.* [49••] reexamined the effects of NP size and surface chemistry on magnetic properties by comparing proton relaxivity data for 10 and 30 nm NPs and for the different surface coatings. Certain MNPs coated with different layers show substantial variation in proton relaxivity. Tong *et al.* [50••] varied the shell/core ratio and showed that an impermeable polymer-coated MNP system exhibited distinctly different T_2 relaxivities even if their core sizes were similar. The T_2 relaxivity of the 14 nm SPIOs increased 2.54-folds when the PEG molecular weight was decreased from 5000 to 1000 Da. SPIOs prepared with a 14 nm core and coated with DSPE-PEG1000 show T_2 relaxivity of

385 mM^{-1} s^{-1}. Surface coating can affect MNP Brownian relaxation in various medium and can also be a 'bridge' to transfer heat into the medium. Liu *et al.* [51••] reported that fine-tuning the surface coating molecular weight (poly(ethylene glycol) methyl ether 2000 (mPEG2000), mPEG5000, and mPEG20000), the SAR is different. The SAR could be significantly increased by 2.5-folds for 19 nm Fe_3O_4 core when surface coating molecular weight decreased from 5000 to 2000. The highest SAR is 930 W/g, which is achieved by 19 nm MNPs coated with mPEG2000.

Conclusion

Numerous efforts have been dedicated to preparing various MNPs for biomedical applications, but optimizing MNP-based nanoagents for early diagnosis and efficient therapeutics is still far from being accomplished. Improving the contrast between pathogenic targets and normal tissues in MRI and maximizing the SAR in hyperthermia remain the most challenging tasks. Recent advancement in the development of novel magnetic nanoparticle platform manifest that the size, shape, composition, and surface-coating dependences should all be examined together in order to reach a comprehensive, conclusive understanding of MNPs and maximize T_1 or T_2 relaxivity and SAR to chemically engineer an ideal nanoagent. However, a number of critical issues should be addressed before this can be actually achieved: first, computational investigation of nucleation process and chemisorption behavior, which have not been well-studied probably due to complex structure of fcc metal ferrites, is imperative to devise and realize the controlled growth of magnetic nanoparticles; second, metabolic behavior, *in vivo* and *in vitro* targeting efficiency of MNP agents and their toxicology need to be addressed for the medical translation of MNP from bench to bed; third, the impacts of interparticle interaction, inorganic–organic core–shell interface, and possible synergistic effects on their application performance should be understood in large degree. Additionally, advanced synthesis methods for large-scale (subkilogram range), high-throughput, highly reproducible industrial monodisperse MNP production is also strongly desirable. Despite these numerous challenges, with a multidisciplinary approach in which the other researchers in chemistry, physics, biology and materials science are involved, we can envisage that MNPs agent will achieve the high sensitivity and efficacy for clinic diagnostics and therapeutics in the future.

Recommended reading

Papers of particular interest, published within the period of review, have been highlighted as:

- • of special interest
- •• of outstanding interest

Acknowledgements

This work was financially supported by the National Natural Science Foundation of China (Grant Nos. 21006079 and 21376192), the Research Fund for the Doctoral Program of Higher Education China (Grant No. 20126101110017).

References and recommended reading

Papers of particular interest, published within the period of review, have been highlighted as:

- • of special interest
- •• of outstanding interest

1. Fan HM, Olivo M: **Magnetic nanorings and nanotubes for cancer detection and therapy**. In *Nanomedicine and Cancer*Srirajaskanthan R, Preedy VRCRS Press; 2012:183-203.

2. Yoo D, Lee JH, Shin TH, Cheon J: **Theranostic magnetic nanoparticles**. *Acc Chem Res* 2011, **44**:863-874.

3. Lacroix LM, Ho D, Sun S: **Magnetic nanoparticles as both imaging probes and therapeutic agents**. *Curr Top Med Chem* 2010, **10**:1184-1197.

4. Ho D, Sun X, Sun S: **Monodisperse magnetic nanoparticles for theranostic applications**. *Acc Chem Res* 2011, **44**:875-882.

5. • Rosensweig RE: **Heating magnetic fluid with alternating magnetic field**. *J Magn Magn Mater* 2002, **252**:370-374.
The author utilized a very interesting methodology to formulate and compute the heating rates of samples subjected to an alternating magnetic field.

6. Thomas LA, Dekker L, Kallumadil M, Southern P, Wilson M, Nair SP, Pankhurst QA, Parkin IP: **Carboxylic acid-stabilised iron oxide nanoparticles for use in magnetic hyperthermia**. *J Mater Chem* 2009, **19**:6529-6535.

7. Hergt R, Dutz S: **Magnetic particle hyperthermia-biophysical limitations of a visionary tumour therapy**. *J Magn Magn Mater* 2007, **311**:187-192.

8. Wang X, Tang J, Shi L: **Induction heating of magnetic fluids for hyperthermia treatment**. *IEEE Trans Magn* 2010, **46**:1043-1051.

9. Warner S: **Diagnostics plus therapy = theranostics**. *Scientist* 2004, **18**:38-39.

10. •• Lee JH, Huh YM, Jun YW, Seo JW, Jang JT, Song HT, Cheon J: **Artificially engineered magnetic nanoparticles for ultrasensitive molecular imaging**. *Nat Med* 2006, **13**:95-99.
The authors developed ultrasensitive MR probe systems based on magnetism-engineered iron oxide (MnMEIO) nanoparticles. In particular, molecular probes based on MnMEIO nanoparticles, which have strong magnetic properties, showed considerably enhanced sensitivity for detecting cancer cells and also made the *in vivo* imaging of small tumors possible. This concept of artificial engineering is critical for developing highly uniform, biocompatible nanoparticles showing optimal functional properties, which in turn can lead to technological innovations such as nanoprobe systems.

11. Erathodiyil N, Ying JY: **Functionalization of inorganic nanoparticles for bioimaging applications**. *Acc Chem Res* 2011, **44**:925-935.

12. Amstad E, Gillich T, Bilecka I, Textor M, Reimhult E: **Ultrastable iron oxide nanoparticle colloidal suspensions using dispersants with catechol-derived anchor groups**. *Nano Lett* 2009, **9**:4042-4048.

13. Jiang WQ, Yang HC, Yang SY, Horng HE, Hung JC, Chen YC, Hong CY: **Preparation and properties of superparamagnetic nanoparticles with narrow size distribution and biocompatible**. *J Magn Magn Mater* 2004, **283**:210-214.

14. Dacoata GM, Degrave E, Debakker PMA, Vandenberghe RE: **Synthesis and characterization of some iron oxides by sol–gel method**. *J Solid State Chem* 1994, **113**:405-412.

15. Deng Y, Wang L, Yang W, Fu S, Elaissari A: **Preparation of magnetic polymeric particles via inverse microemulsion polymerization process**. *J Magn Magn Mater* 2003, **257**:69-78.

16. Abu Mukh-Qasem A, Gedanken A: **Sonochemical synthesis of stable hydrosol of Fe_3O_4 nanoparticles**. *J Colloid Interface Sci* 2005, **284**:489-494.

17. Chen D, Xu R: **Hydrothermal synthesis and characterization of nanocrystalline Fe_3O_4 powders**. *Mater Res Bull* 1998, **33**:1015-1021.

18. •• Hyeon T, Lee SS, Park J, Chung Y, Na HB: **Synthesis of highly crystalline and monodisperse maghemite nanocrystallites without a size-selection process**. *J Am Chem Soc* 2001, **123**:12798-12801.
This article describes how highly crystalline, monodisperse γ-Fe_2O_3 nanocrystallites were fabricated from the controlled oxidation of uniform iron nanoparticles produced by thermally decomposing an iron complex. The nanoparticles were directly obtained using this method without requiring further size adjustment. The size of the nanoparticles was easily and reproducibly tuned by changing the experimental parameters. In addition, the nanoparticle yield was over 80%, indicating that the process is readily scalable.

19. Zeng LY, Ren WZ, Zheng JJ, Cui P, Wu AG: **Ultrasmall water-soluble metal-iron oxide nanoparticles as T_1-weighted contrast agents for magnetic resonance imaging**. *Phys Chem Chem Phys* 2012, **14**:2631-2636.

20. Veintemillas-Verdaguer S, Morales MP, Serna CJ: **Continuous production of γ-Fe_2O_3 ultrafine powders by laser pyrolysis**. *Mater Lett* 1998, **35**:227-231.

21. Yosida K: **Theory of magnetism**. *Solid-State Sciences*. 1996.

22. Cullity BD: *Introduction to Magnetic Materials*. Reading, MA: Addison Wesley Publishing Company; 1972, .

23. Unruh KM, Chien CL: In *Nanomaterials: Synthesis Properties and Applications*Edelstein AS, Cammarata RCBristol, U.K: Institute of Physics Publishing; 1996. Ch. 14.

24. Matsumoto Y, Jasanoff A: **T_2 relaxation induced by clusters of superparamagnetic nanoparticles: Monte Carlo simulations**. *Magn Res Imaging* 2008, **26**:994-998.

25. Park J, An K, Hwang Y, Park JG, Noh HJ, Kim JY, Park JH, Hwang HM, Hyeon T: **Ultra-large-scale syntheses of monodisperse nanocrystals**. *Nat Mater* 2004, **3**:891-895.

26. Sun SH, Zeng H, Robinson DB, Raoux S, Rice PM, Wang SX, Li G: **Monodisperse $MFe_2O_{4;1;}$ (M = Fe, Co, Mn) nanoparticles**. *J Am Chem Soc* 2004, **126**:273-279.

27. Choo ESG, Tang XS, Sheng Y, Xue JM: **Controlled loading of superparamagnetic nanoparticles in fluorescent nanogels as effective T_2-weighted MRI contrast agents**. *J Mater Chem* 2011, **21**:2310-2319.

28. •• Kim BH, Lee N, Kim H, An K, Park YI, Choi Y, Hyeon T: **Large-scale synthesis of uniform and extremely small-sized iron oxide nanoparticles for high-resolution T_1 magnetic resonance imaging contrast agents**. *J Am Chem Soc* 2011, **133(32)**:12624-12631.
Uniform, extremely small (<4-nm-diameter) iron-oxide nanoparticles (ESIONs) were synthesized by heating an iron-oleate complex in oleyl alcohol to control how the complex thermally decomposed. The obtained ESIONs, whose surfaces showed numerous Fe^{3+} ions with 5 unpaired electrons, exhibited high r_1 relaxivities (>4.7 mM^{-1} s^{-1}) and low r_2/r_1 ratios (<6.2), demonstrating that ESIONs could be used as efficient T_1 contrast agents. ESIONs showing high r_1 relaxivity and long blood circulation time enabled the high-resolution blood pool T_1-weighted magnetic resonance imaging (MRI) of various ≥0.2-mm-diameter blood vessels.

29. •• Tromsdorf UI, Bruns OT, Salmen SC, Beisiegel U, Weller H: **A highly effective, nontoxic T_1 MR contrast agent based on ultrasmall PEGylated iron oxide nanoparticles**. *Nano Lett* 2009, **9**:4434-4440.
The authors systematically developed a potential MR T_1 contrast agent based on very small polyethylene glycosylated (PEGylated) iron oxide nanoparticles. The as-developed contrast agent showed the lowest r_2/r_1 ratio (2.4) at 1.41 T reported to date for PEGylated iron oxide nanoparticles and an r_1 relaxivity (7.3 mM^{-1} s^{-1}) two times higher than Magnevist®, a typical gadolinium-based T_1 contrast agent used as a clinical standard. For all the parameters tested, it showed the highest stability and suitable relaxometric properties, the lowest cytotoxicity, and the lowest uptake into macrophages.

30. • Carrey J, Mehdaoui B, Respaud M: **Simple models for dynamic hysteresis loop calculations of magnetic single-domain nanoparticles: application to magnetic hyperthermia optimization**. *J Appl Phys* 2011, **109**:083921.
The authors studied the three types of theories suitable for describing hysteresis loops of MNPs equilibrium functions, Stoner–Wohlfarth model based theories (SWMBTs), and a linear response theory (LRT) using the Néel–Brown relaxation time. The results show that LRT is only pertinent for MNPs with strong anisotropy and that SWMBTs should be used for weakly anisotropic MNPs. The optimum volume of MNPs for magnetic hyperthermia is derived as a function of material and experimental parameters.

31. Chen S, Chiang CL, Hsieh SC: **Simulating physiological conditions to evaluate nanoparticles for magnetic fluid hyperthermia (MFH) therapy applications**. *J Magn Magn Mater* 2010, **322**:247-252.

32. Fortin JP, Wilhelm C, Servais J, Ménager C, Bacri JC, Gazeau F: **Size-sorted anionic iron oxide nanomagnets as colloidal mediators for magnetic hyperthermia**. *J Am Chem Soc* 2007, **129**:2628-2635.

33. Liu XL, Choo SGE, Ahmed AS, Zhao LY, Yang Y, Ramanujan RV, Xue JM, Fan DD, Fan HM, Ding J: **Magnetic nanoparticles-loaded polymer nanospheres as magnetic hyperthermia agent**. *J Mater Chem B* 2014, **2**:120-128.

34. Fan HM, You GJ, Li Y, Zheng Z, Tan HR, Shen ZX, Tang SH, Feng YP: **Shape-controlled synthesis of single-crystalline Fe_2O_3 hollow nanocrystals and their tunable optical properties**. *J Phys Chem C* 2009, **113**:9928-9935.

35. Fan HM, Yi JB, Yang Y, Kho KW, Tan HR, Shen ZX, Ding J, Sun XW, Olivo MC, Feng YP: **Single-crystalline MFe_2O_4 nanotubes/nanorings synthesized by thermal transformation process for biological applications**. *ACS Nano* 2009, **3**:2798-2808.

36. Liu XL, Zheng MR, Lv YB, Fang J, Sow CH, Fan HM, Ding J: **Large-scale synthesis of high-content Fe nanotubes/nanorings with high magnetization by H_2 reduction process**. *Mater Res Bull* 2013, **48**:5003-5007.

37. Li SP, Peyrade D, Natali M, Lebib A, Chen Y, Ebels U, Buda LD, Ounadjela K: **Flux closure structures in cobalt rings**. *Phys Rev Lett* 2001, **86**:1102.

38. •• Fan HM, Olivo M, Shuter B, Yi JB, Bhuvaneswari R, Tan HR, Xing GC, Ng CT, Liu L, Lucky SS, Bay BH, Ding J: **Quantum dot capped magnetite nanorings as high performance nanoprobe for multiphoton fluorescence and magnetic resonance imaging**. *J Am Chem Soc* 2010, **132**:14803-14811.
The authors developed a class of magnetic-fluorescent nanoprobes whose magnetic vortex was a core capped with highly luminescent quantum dots (QDs). The obtained biocompatible multicolor QD-capped magnetite nanorings (NRs) exhibited much stronger magnetic resonance (MR) T_2^* than commercial superparamagnetic iron oxide (i.e. the r_2^* relaxivity and r_2^*/r_1 ratio were 4 and 110 times larger, respectively, than those of commercial superparamagnetic iron oxide). This work showed the great potential of magnetic-vortex-core-based multifunctional nanoparticles as high-performance nanoprobes for biomedical applications.

39. Kim D, Lee N, Park M, Kim BH, An K, Hyeon T: **Synthesis of uniform ferrimagnetic magnetite nanocubes**. *J Am Chem Soc* 2008, **131**:454-455.

40. •• Lee N, Choi Y, Lee Y, Park M, Moon WK, Choi SH, Hyeon T: **Water-dispersible ferrimagnetic iron oxide nanocubes with extremely high r_2 relaxivity for highly sensitive *in vivo* MRI of tumors**. *Nano Lett* 2012, **12**:3127-3131.
The authors achieved the theoretically predicted maximum r_2 relaxivity by optimizing the overall size of ferrimagnetic iron oxide nanoparticles. Uniform iron oxide nanocubes, whose edges were 22 nm long, were encapsulated with PEG-phospholipids and exhibited high colloidal stability in aqueous media. Tumors were MR imaged *in vivo* using a clinical 3 T MR scanner when the nanocubes were intravenously injected into a patient.

41. •• Guardia P, Di Corato R, Lartigue L, Wilhelm C, Espinosa A, Garcia-Hernandez M, Pellegrino T: **Water-soluble iron oxide nanocubes with high values of specific absorption rate for cancer cell hyperthermia treatment**. *ACS Nano* 2012, **6**:3080-3091.
The authors reported the specific absorption rates (SARs) for 13–40-nm-diameter water-soluble cubic iron oxide nanocrystals (IONCs) prepared

using one-pot synthesis. Among the various sizes of IONCs tested, those whose average diameter was 19 ± 3 nm showed significant SARs under clinical conditions and reached SARs up to 2452 W g^{-1} Fe at 520 kHz and 29 kA m^{-1}, which is one of the highest SARs reported to date for IONCs.

42. •• Jang JT, Nah H, Lee JH, Moon SH, Kim MG, Cheon J: **Critical enhancements of MRI contrast and hyperthermic effects by dopant-controlled magnetic nanoparticles**. *Angew Chem Int Edit* 2009, **121**:1260-1264.

The authors demonstrated that the magnetism of highly magnetic metal ferrite nanoparticles can be very effectively modulated by tuning the concentration of Zn^{2+} dopant in the nanoparticles, which acted as MR-contrast and hyperthermia agents showing r_2 relaxivities 8–14 times greater for MRIs and SLPs four times greater for hyperthermia cancer cell treatments than conventional nanoparticle agents. In addition, their nanoparticles were nontoxic. Such high-performance magnetic nanoparticles fabricated using this method of engineering magnetism could play a significant role in improving current diagnostic and therapeutic methods and other biomedical studies such as cell actuation.

43. • Zeng H, Li J, Wang ZL, Liu JP, Sun S: **Bimagnetic core/shell $FePt/Fe_3O_4$ nanoparticles**. *Nano Lett* 2004, **4**:187-190.

Bimagnetic core/shell $Fe_{58}Pt_{42}/Fe_3O_4$ nanoparticles were synthesized by spraying a high-temperature solution to coat a Fe_3O_4 shell onto a 4-nm-diameter $Fe_{58}Pt_{42}$ core. The shell thickness was tunable from 0.5 to 3 nm. The authors mainly investigated the magnetic properties of the as-synthesized core/shell particles, which depended on the shell thickness because of the exchange coupling between the core and shell.

44. •• Lee JH, Jang JT, Choi JS, Moon SH, Noh SH, Kim JW, Cheon J: **Exchange-coupled magnetic nanoparticles for efficient heat induction**. *Nat Nanotechnol* 2011, **6**:418-422.

The authors developed exchange-coupled magnetic nanoparticles as a method of modulating magnetism, which significantly enhanced the magnetic heat induction of the nanoparticles. The authors used the exchange-coupling between a magnetically hard core and a magnetically soft shell to tune the magnetic properties of the nanoparticles and maximize the specific loss power, which is a gauge of conversion efficiency. The optimized core-shell magnetic nanoparticles showed specific loss powers an order of magnitude larger than those of conventional iron-oxide nanoparticles. The nanoparticles showed antitumor activity in mice and therapeutic efficacy superior to that of a common anticancer drug.

45. Suh WH, Suslick KS, Stucky GD, Suh YH: **Nanotechnology, nanotoxicology, and neuroscience**. *Prog Neurobiol* 2009, **87**:133-170.

46. Xie J, Xu C, Kohler N, Hou Y, Sun S: **Controlled PEGylation of monodisperse Fe_3O_4 nanoparticles for reduced non-specific uptake by macrophage cells**. *Adv Mater* 2007, **19**:3163-3166.

47. Lin CL, Lee CF, Chiu WY: **Preparation and properties of poly (acrylic acid) oligomer stabilized superparamagnetic ferrofluid**. *J Colloid Interface Sci* 2005, **291**:411-420.

48. Sudimack J, Lee RJ: **Targeted drug delivery via the folate receptor**. *Adv Drug Del Rev* 2000, **41**:147-162.

49. •• Duan H, Kuang M, Wang X, Wang YA, Mao H, Nie S: **Reexamining the effects of particle size and surface chemistry on the magnetic properties of iron oxide nanocrystals: new insights into spin disorder and proton relaxivity**. *J Phys Chem C* 2008, **112**:8127-8131.

The authors compared proton relaxivity data for two nanoparticle sizes and three surface coatings to re-examine the effects of nanoparticle size and surface chemistry on the magnetic properties of iron oxide nanocrystals. The measured proton relaxation rates strongly depended on the particle size, the coating layer hydrophilicity, and the coordination chemistry of the inner capping ligands.

50. •• Tong S, Tong S, Hou S, Zheng Z, Zhou J, Bao G: **Coating optimization of superparamagnetic iron oxide nanoparticles for high T_2 relaxivity**. *Nano Lett* 2010, **10**:4607-4613.

This paper describes a new method of coating superparamagnetic iron oxide nanoparticles (SPIOs) and demonstrates that the T_2 relaxivity per nanoparticle can be increased >200-fold by fine-tuning the core size of and the PEG coating on the surface of the SPIOs. *In vivo* tumor imaging results demonstrated the potential of the SPIOs for clinical applications.

51. •• Liu XL, Fan HM, Yi JB, Yang Y, Choo ESG, Xue JM, Ding J: **Optimization of surface coating on Fe_3O_4 nanoparticles for high performance magnetic hyperthermia agents**. *J Mater Chem* 2012, **22**:8235-8244.

The authors demonstrated a general strategy of optimizing biocompatible surface coatings for designing and developing magnetic-nanoparticle-based hyperthermia agents. The SAR of the nanoparticles was significantly increased (to 74%) by fine-tuning the surface coating for an optimal magnetic core size, and the nanoparticles showed very small (<5%) variation in saturation magnetization. The effect of surface coating on SAR mainly results from Brownian loss, thermal conductivity, and colloid stability on SAR.

52. Li X, Qian Y, Liu T, Hu X, Zhang G, You Y, Liu S: **Amphiphilic multiarm star block copolymer-based multifunctional unimolecular micelles for cancer targeted drug delivery and MR imaging**. *Biomaterials* 2011, **32**:6595-6605.

53. Lamanna G, Kueny-Stotz M, Mamlouk-Chaouachi H, Ghobril C, Basly B, Bertin A, Felder-Flesch D: **Dendronized iron oxide nanoparticles for multimodal imaging**. *Biomaterials* 2011, **32**:8562-8573.

54. Tromsdorf UI, Bigall NC, Kaul MG, Bruns OT, Nikolic MS, Mollwitz B, Weller H: **Size and surface effects on the MRI relaxivity of manganese ferrite nanoparticle contrast agents**. *Nano Lett* 2007, **7**:2422-2427.

55. Barick KC, Aslam M, Lin YP, Bahadur D, Prasad PV, Dravid VP: **Novel and efficient MR active aqueous colloidal Fe_3O_4 nanoassemblies**. *J Mater Chem* 2009, **19**:7023-7029.

56. Yang Y, Liu XL, Yi JB, Yang Y, Fan HM, Ding J: **Stable vortex magnetite nanorings colloid: micromagnetic simulation and experimental demonstration**. *J Appl Phys* 2012, **111**:044303.

57. Noh SH, Na W, Jang JT, Lee JH, Lee EJ, Moon SH, Cheon J: **Nanoscale magnetism control via surface and exchange anisotropy for optimized ferrimagnetic hysteresis**. *Nano Lett* 2012, **12**:3716-3721.